Low-frequency pulsations in a He-Xe laser with several transverse modes: Experimental and numerical studies

H. Lin
Department of Physics and Astronomy, Bates College, Lewiston, Maine 04240

N. B. Abraham
Department of Physics, Bryn Mawr College, 101 North Merion Avenue, Bryn Mawr, Pennsylvania 19010-2899
(Received 29 September 1993)

Spatial pattern pulsations are observed at frequencies much less than the intermode beat frequencies in a He-Xe laser operating at 3.51 μm. Numerical studies indicate that such low-frequency pulsations can arise from secondary beat notes between the frequencies of unequally spaced modes. The decay rate of the active medium is an important parameter which sets the scale for mode pulling without locking, which leads to these pulsations.

PACS number(s): 42.60.Mi, 42.50.Ne

I. INTRODUCTION

A multi-transverse-mode laser is a typical nonlinear optical system with a rich set of dynamical behaviors which have been observed experimentally and studied theoretically for many years. Many efforts have been made to model such lasers by studying the instabilities and dynamics caused by interactions between modes and the active medium or by spatial inhomogeneity in the gain and external pumping [1–13]. Similar to a multi-longitudinal-mode laser, a multi-transverse-mode laser may pulse periodically or chaotically [14–16] for reasons related to primary and secondary beat frequencies. However, corresponding changes in transverse spatial patterns cannot be neglected as an important feature causing the dynamics. Sometimes the transverse pattern pulses with time; in other cases there may be a stationary spatial distribution having a single optical frequency but involving spatial parts of many cavity modes [17–27].

We have used a He-Xe laser with several transverse modes to study spatiotemporal dynamics of laser transverse patterns. In our observations, many states which might be termed "single-mode" based on the constant intensity observed experimentally are actually "cooperative frequency locked" (CFL) states, as termed by Lugiato, Oldano, and Narducci [8]. That is, there is a single lasing frequency but the transverse pattern is not close to that of any cavity mode. We think, rather, that while this can be regarded as a "frequency-pulling" effect, the CFL state is actually a nonlinear mode, that is, a nonlinear distortion of a cavity mode, or what might be called a spatially "dressed-mode." For some values of the control parameters, supermode beating [11] (beating of two nonlinear modes) is observed. For other parameters, the laser pulses at frequencies much less than the intermode beat frequencies. Similar low-frequency pulsations have also been observed in other lasers. For instance, the typical frequency is about 10–20 MHz in a 3.39-μm He-Ne laser [28], and 2 MHz in a CO_2 laser [29].

Numerical simulations using a simple model of transverse patterns have been done to study the physical processes that can lead to these low-frequency pulsations. The results show that some low-frequency pulsations are caused by the unlocking of the spacings between the lasing modes and that the decay rate of the atomic population difference and the nonequidistancy of the frequency spacings of the cavity modes are important factors in the occurence of low-frequency pulsations.

Our experimental results and numerical simulations are given in Secs. II and III, respectively. Section IV provides a further discussion of the results and conclusions.

II. EXPERIMENTAL RESULTS

Our experimental setup is shown schematically in Fig. 1. The experimental laser is a He-Xe laser operating on the 3.51-μm transition of neutral xenon in a Fabry-Pérot cavity geometry. The inner diameter of the discharge tube is 4 mm and the active region of the discharge is 12-cm long; the dc discharge in the medium is excited in a cold-cathode design. The pressure of xenon used in our experiments was 175 mTorr. The pressure of helium was changed to get different ratios of the homogeneous to inhomogeneous linewidths. The typical ratio of homogeneously broadened and inhomogeneously broadened linewidths is 1:1.48 for our operating pressures. The typical linewidth of the gain curve is 145 ± 11 MHz. The mode pulling of lasing frequencies from their corresponding cavity-mode eigenfrequencies varies with the detuning of the mode from the center frequency of the gain line shape due to inhomogeneous broadening. Our measurements show that the mode-pulling factor is about 2–3 in the experimental laser. The cavity length is 27.5 cm. The output coupler is a plane mirror of reflectivity 90%. The second surface of the mirror is uncoated and has a 30′ wedge angle. The radius of curvature of the other mirror, a totally reflecting spherical mirror, is 60 cm. Its longitudinal position can be slightly adjusted by a piezoelectric crystal (PZT) attached to it.

The resonant frequency of a Gaussian-Lagurre eigen-

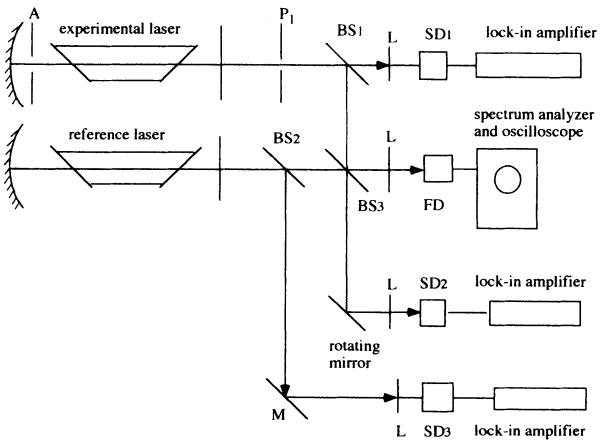

FIG. 1. Experimental setup. L: lenses; BS_i, beam splitters; SD_i; slow photodetectors; FD_i, fast photodetectors; A: intracavity aperture; P_1, a pinhole which can be scanned across the laser beam.

mode of an empty Fabry-Pérot cavity having cylindrical symmetry is [30].

$$\nu_{q,p,m}=(c/2L)\{q+(2p+m+1)\cos^{-1}[(g_1g_2)^{1/2}]/\pi\} ,$$

where q, p, and m are indices of modes (q represents the qth longitudinal mode; one pair of p and m correspond to an eigenmode transverse pattern. The parameter $g_i=1-L/R_i$, $i=1,2$, where R_1 and R_2 are the radii of curvature of the two mirrors of the cavity, respectively, and L is the length of the cavity). For our laser the cavity frequency spacing between adjacent longitudinal modes, $\Delta\nu_L$, is 546 MHz and the cavity frequency spacing between adjacent transverse modes of one longitudinal mode, $\Delta\nu_T$, is 129 MHz. Under these conditions, the laser is more likely to operate on a single longitudinal mode and its higher-order transverse modes.

An intracavity pinhole is placed near the spherical mirror. The Fresnel number of the cavity, F (which is proportional to d^2L, where d is the diameter of the effective area of the reflector), is changed by changing the diameter of this pinhole. The output signal is split into two parts by beamsplitter BS_1. One part is optically chopped and then focused by a lens on an InAs photodiode, SD_1; the photovoltage is fed to a lock-in amplifier for observation of the relative total power, which can be recorded by an X-Y recorder. P_1 is a pinhole of diameter 0.3 mm which can be scanned across the beam to get a one-dimensional near-field transverse pattern. It is placed 10 cm away from the output mirror. Another part of the signal is sent to a fast photodetector, FD, whose frequency response ranges from 1 kHz to 100 MHz. The homodyne power spectrum of the experimental laser is observed by feeding the output of the FD to a radio-frequency spectrum analyzer and a fast oscilloscope. A stabilized single-mode He-Xe standing-wave laser is used as a reference laser and its intensity is monitored by photodetector SD_3. The beat notes between the experimental laser and the reference laser can be observed in the heterodyne portion of the power spectrum of the signal from detector FD. A rotating mirror and another photodiode, SD_2, are used to observe the far-field transverse pattern of the laser.

For a fixed excitation current i, the transverse pattern and the temporal behavior of the laser strongly depend on the Fresnel number. When the diameter of the intracavity pinhole is small ($d=1.5$ mm), the laser is in single-mode operation. (Here we use the experimental meaning of the term "single-mode," namely, a lasing state that has a single optical frequency and a stationary transverse intensity pattern.) As the cavity detuning is varied, the output power is changed but the profile of the transverse pattern remains nearly the same. Nevertheless, under these conditions, the transverse pattern of the lasing mode may be or may not be close to that of a cavity mode. For the latter case, the lasing mode is a nonlinear mode (CFL state). Figure 2(a) is the transverse pattern of the lasing mode for $i=3.5$ mA, which is obviously not a pure Gaussian mode.

As the diameter of the intracavity pinhole is increased ($d\geq 2.0$ mm), the laser switches from one transverse mode to another as the cavity is detuned. The one-dimensional transverse patterns of these lasing modes often have different symmetries, as illustrated in the sequence from Fig. 2(b) to Fig. 2(d). The output intensity may pulse for some cavity detunings. One type of frequency f, in homodyne spectra are of the order of 90 MHz, as shown in Fig. 3. Two heterodyne beat notes ν_{B1} and ν_{B2} can be observed and $|\nu_{B1}-\nu_{B2}|=f$. This indi-

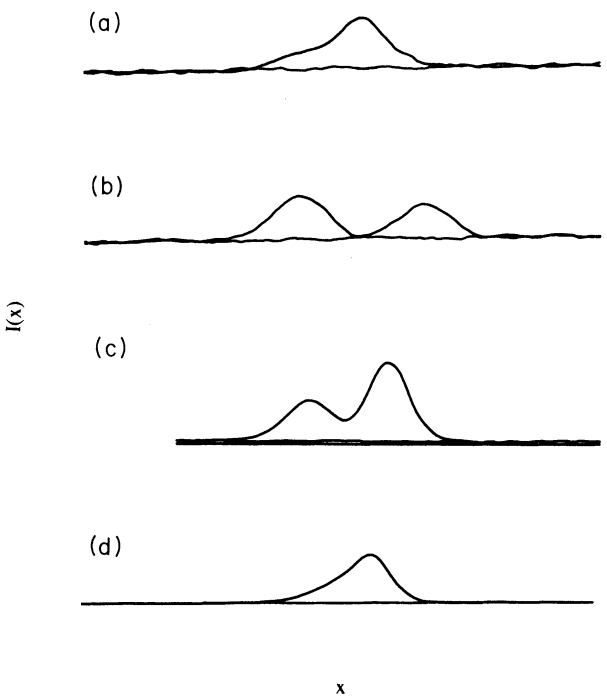

FIG. 2. (a) One-dimensional transverse intensity pattern which is obtained by scanning P_1 along the x axis for $d=1.5$ mm and $i=3.5$ mA. (b)–(d) Transverse intensity patterns of three different modes as the cavity is detuned for one free spectral range for $d=2.5$ mm and $i=3.5$ mA. The vertical scales of (c) and (d) are decreased by a factor of 2.5 and a factor of 10, respectively.

cates that two modes are lasing simultaneously and f is caused by the beating of these two lasing modes. The values of f is 85 MHz in Fig. 3(a) and 90 MHz in Fig. 3(b). This is caused by detuning-dependent mode pulling in the inhomogeneously broadened medium. We measured the mode-pulling curve and calculated the corresponding cavity frequency spacing between the two beating modes. The results show that the empty cavity frequency spacing is 248±20 MHz. Given that we calculate the longitudinal and transverse mode spacings to be $\Delta\nu_L = 546$ MHz and $\Delta\nu_T = 258$ MHz, respectively, we conclude that this intermode frequency is due to beating of two transverse modes. The two corresponding cavity modes may be either modes (q,p,m) and $(q,p,m+2)$ or (q,p,m) and $(q,p+1,m)$. For the first case, a breaking of the cylindrical symmetry happens; for the second one, there is no symmetry breaking. From the spatial patterns we obtained, however, it is not clear which case is dominant. We have also considered the possibility that the observed signal comes from the beating of two modes belonging to different longitudinal modes, such as modes $(q,0,0)$ and $(q-1,1,0)$. The cavity frequency spacing between such modes is 288 MHz. Thus, within our experimental uncertainty, this possibility seems to be excluded.

Another type of observed pulsation has frequencies of the order of 4 MHz and its harmonics and subharmonics, which are much lower than the smallest cavity-mode frequency spacings. These low-frequency pulsations may be periodic, quasiperiodic, or irregular. Sometimes low-frequency pulsing and intermode beating appear simultaneously; sometimes only low-frequency pulsing is observed. Even when the excitation current is decreased, such low-frequency pulsations can still be observed as the transverse pattern of the beam changes from one to another. On the other hand, when the Fresnel number of the cavity is small and the cavity supports only one transverse mode, this type of pulsation has not been observed. This suggests that the low-frequency pulsations may result from interactions among transverse modes.

Some examples of low-frequency pulsations are illus-

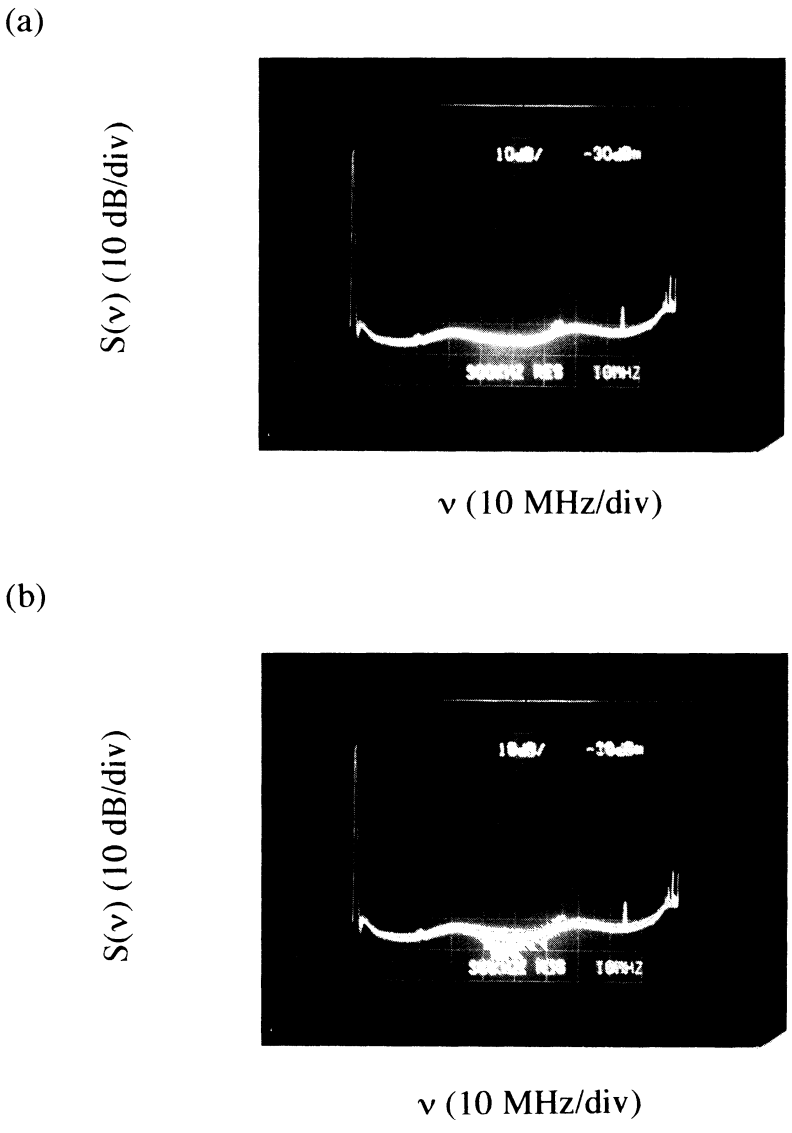

FIG. 3. Examples of homodyne and heterodyne spectra of intermode beating of the laser. (a) The intermode beat frequency (sharper peak) $f = 90$ MHz and the two heterodyne beat nets ν_{B1} and ν_{B2} are -34 and 56 MHz, respectively. (b) $f = 85$ MHz; ν_{B1} and ν_{B2} are -65 and 20 MHz, respectively. Horizontally, one grid in the picture is 10 MHz. The peaks at 100 MHz are due to electronic noise.

trated in Fig. 4. In Fig. 4(a), there are two groups of homodyne frequencies and three heterodyne beat notes. One group of homodyne frequencies are 3 and 6 MHz; the other group includes 87 and 90 MHz. We assume these represent beats between three modes spaced successively by 87 and 90 MHz. The beat frequency between the two extreme modes would be weaker and would occur at 177 MHz, beyond the response of our detector-amplifier combination. The low frequencies may be the result of secondary beat frequencies as follows. Three heterodyne beat notes are observed at 14, 17, and 73 MHz. This indicates that the cavity supports three modes which lase simultaneously. We interpret these to mean that relative to the reference laser one mode is at -73 MHz, one is at 14 MHz, and a third is at 104 MHz (also beyond the range of our system response). Suppose that their frequencies are labeled ω_{i-1}, ω_i, and ω_{i+1}, respectively. When ω_i is not at the center of the gain curve, there is a small difference δ between $(\omega_{i+1}-\omega_i)$ and $(\omega_i-\omega_{i-1})$ [$\delta=|(\omega_{i+1}-\omega_i)-(\omega_i-\omega_{i-1})|$ and $\delta\ll(\omega_i-\omega_{i-1})$ or $(\omega_{i+1}-\omega_i)$] because of detuning-dependent mode pulling. The nonlinear response of the medium then generates both AM and FM modulation of each mode and of the total intensity at frequency δ. Hence one group of homodyne frequencies are at $\delta, 2\delta, \ldots$ and the other group of frequencies are at $(\omega_i-\omega_{i-1})\pm\delta, (\omega_i-\omega_{i-1})\pm 2\delta, \ldots$. The smaller sideband peak at 17 MHz indicates the AM and FM modulation of the mode at 14 MHz. One can also interpret the peak at 17 MHz as resulting from the third-order nonlinearity of the medium which generates the optical combination tone represented by $\omega_{i-1}+\omega_{i-1}-\omega_i$. Its beat note with the reference laser would appear at 17 MHz. Beating of the signals at 14 and 17 MHz would modulate the total intensity at 3 MHz. The harmonics of 3 MHz in the observed signal indicate an additional response beyond the generation of the combination tone.

The above analysis is also applicable for Fig. 4(b),

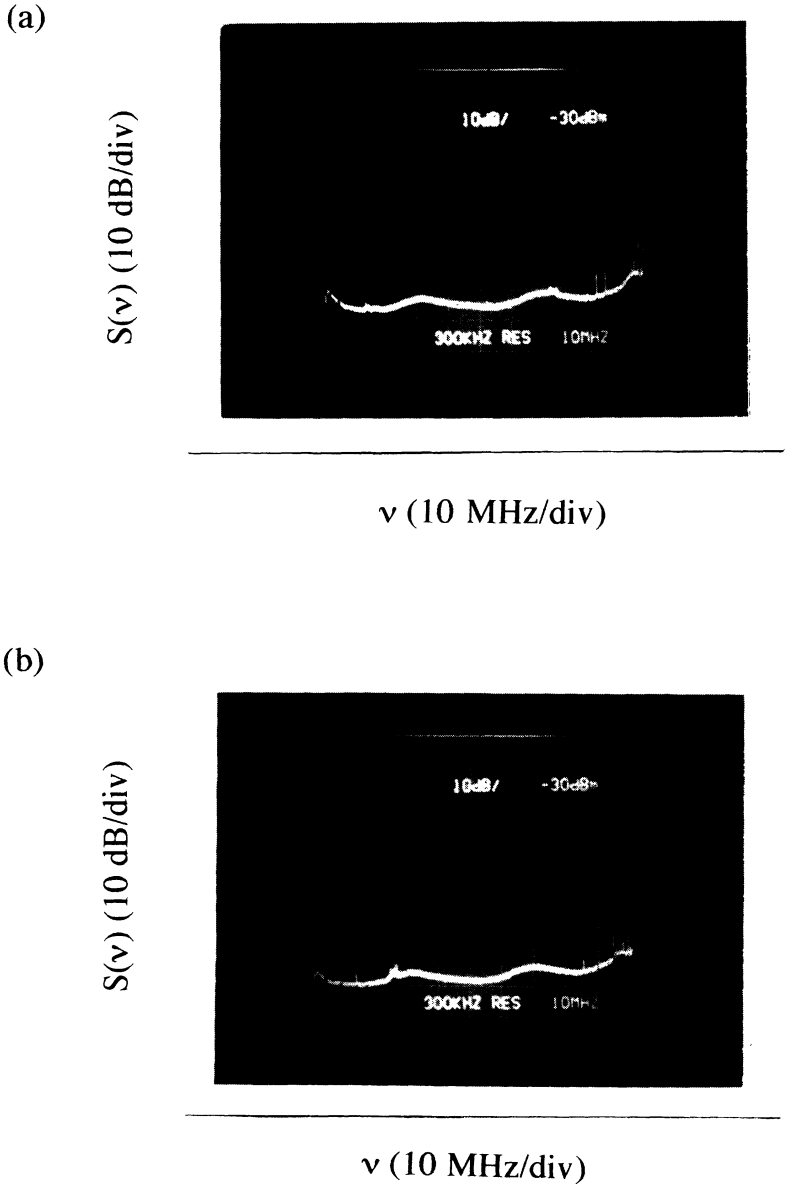

FIG. 4. Examples of homodyne and heterodyne spectra of low-frequency pulsation of the laser. Both low frequencies and intermode beat frequencies can be observed in (a) and (b). There are three heterodyne beat notes in (a), indicating that three modes are lasing. No intermode beat frequencies appear in (c) and (d).

though only one heterodyne beat note is observed. The other beat notes are likely to have been missed due to the limited frequency bandwidth of the detector.

For some periodic low-frequency pulsations as shown in Fig. 4(c), the fundamental frequency increases with excitation current. This increase is illustrated by the data in Table I.

Since it is well known that the Rabi oscillation is one of the driving sources of pulsations in lasers [31], we decided to compare these results with what one might expect from Rabi oscillations induced by the total intensity. Since the power of the laser is proportional to the excitation current within the region we used, the Rabi frequency also increases with the excitation current. We estimate the Rabi frequency in the following way:

TABLE I. Average power and fundamental low frequency of the homodyne spectrum versus excitation current.

i (mA)	P (arb. units)	f (MHz)
1.25	0.85±0.02	4.0±0.5
2.50	3.5±0.2	6.2±0.5
3.75	6.0±0.2	8.0±0.5

$$\Omega=(\gamma\langle I\rangle)^{1/2}$$
$$=(\gamma\langle I_0\rangle)^{1/2}[1+(\langle I\rangle-\langle I_0\rangle)/\langle I_0\rangle]^{1/2}$$
$$=\Omega_0[1+(\langle I\rangle-\langle I_0\rangle)/\langle I_0\rangle]^{1/2}\,, \tag{1}$$

where $\langle I\rangle$ is the total average intensity of the laser.

(c)

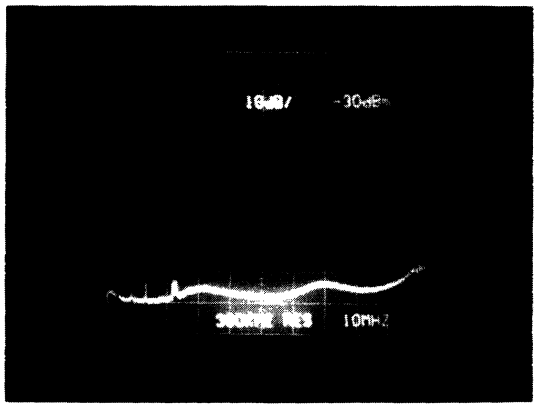

S(ν) (10 dB/div)

ν (10 MHz/div)

FIG. 4. (*Continued*).

(d)

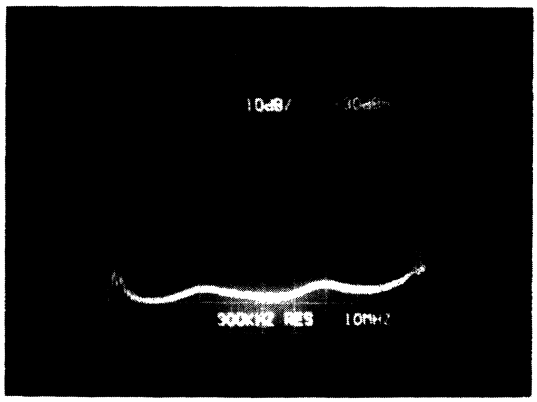

S(ν) (10 dB/div)

ν (10 MHz/div)

$\langle I_0 \rangle$ is a chosen reference intensity and Ω_0 is the reference Rabi frequency.

As the total average intensity is proportional to total power, Eq. (1) can be written as

$$\Omega=\Omega_0[1+(P-P_0)/P_0]^{1/2} , \quad (2)$$

where P and P_0 represent the total power and reference power, respectively. Supposing that the low-frequency pulsation is caused by a Rabi oscillation, we use the total power and the fundamental frequency for $i=1.25$ mA as the reference current and reference Rabi frequency, respectively. The predicted values of Ω versus P and the observed low-frequency values versus P are plotted in Fig. 5. The experimentally observed frequency increases with P approximately linearly while Ω depends on P parabolicly. Hence we conclude the Rabi-oscillation is not a dominant driving source for the low-frequency pulsations we have observed.

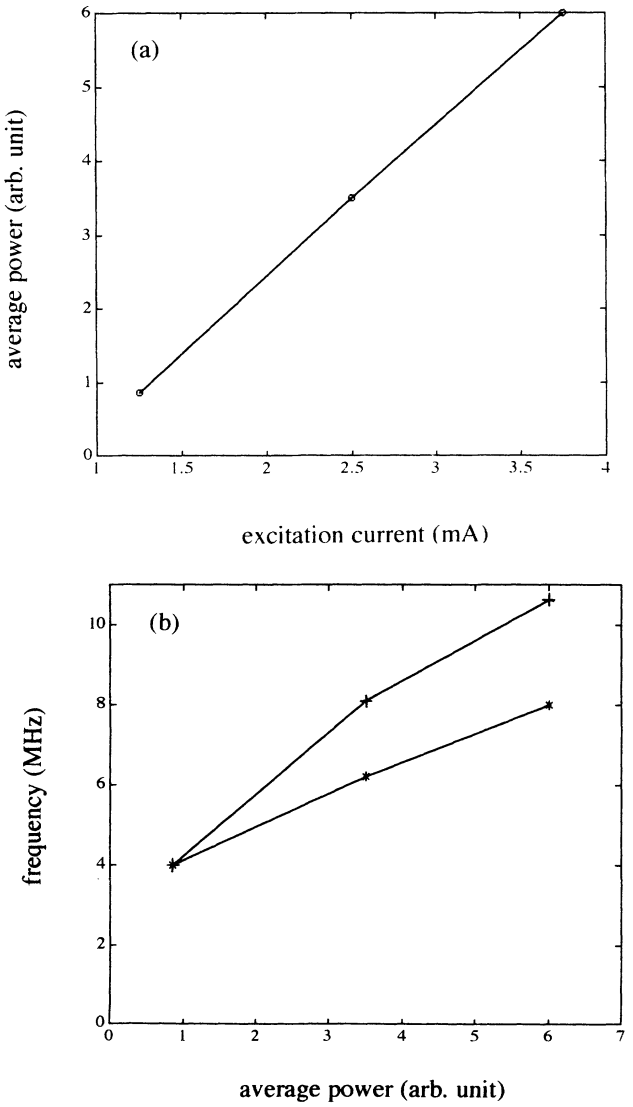

FIG. 5. (a) Average power of the laser vs excitation current. (b) Fundamental frequency symbolized by * and Rabi oscillation frequency symbolized by + vs average power.

Bistability is also observed in our experiments. For example, when the voltage on the PZT, V_{PZT}, is increased, the laser changes from a single-mode state to a low-frequency pulsing state at a certain voltage V_1 and remains in the pulsing state. Then the voltage is decreased. When $V_{PZT}=V_1$, however, the laser does not change back to the single-mode state. It stays in the pulsing state until V is decreased to V_2 ($V_2 \leq V_1$) and then switches to the single-mode state. This is in agreement with a similar bistability observed in Ref. [15].

III. NUMERICAL STUDIES

A. Model

In Refs. [11,12], we used a model of a homogeneously broadened medium and of a cavity with a single transverse dimension to study transverse dynamics of a laser. The cavity configuration of the model, though far from that appropriate to most gas and solid-state lasers, can be regarded as an approximation of a stripe-geometry diode laser or a rectangularly wave-guided laser. The transverse eigenfunctions of this model are cosine functions. It is assumed that frequency spacing between adjacent longitudinal modes, $c/2L$, is much greater than the linewidth of atomic polarization, $\gamma_\perp/\pi$, where $\gamma_\perp$ is the decay rate of the atomic polarization. Hence the cavity can be assumed to support a single longitudinal model and a group of its higher-order transverse modes. The relaxation rate of the population difference is denoted by $\gamma_\parallel$.

The Maxwell-Bloch equations of the model are [8]

$$\frac{\partial E}{\partial t}=-\kappa\left[(1-i\Delta)E-2CP-i\alpha\frac{\partial^2 E}{\partial x^2}\right] ,$$

$$\frac{\partial P}{\partial t}=-\gamma_\perp[(1+i\Delta)P-ED] ,$$

$$\frac{\partial D}{\partial t}=-\gamma_\perp[D-1+\tfrac{1}{2}(E^*P+EP^*)] ,$$

where E is the electric field, P is the atomic polarization, and D is the population inversion, respectively, κ is the cavity linewidth, and $2C$ is the pump parameter. The atomic detuning parameter Δ is given by

$$\Delta=(\omega_a-\omega_{0,r})/\gamma_\perp ,$$

where ω_a is the atomic angular frequency and $\omega_{0,r}$ is the lasing frequency of the fundamental transverse mode ($n=0$).

The angular frequency of the nth transverse cavity mode is given by

$$\omega_{n,c}=\omega_{0,c}+\kappa a\pi^2 n^2 ,$$

where $a=1/(4\pi FT)$ and T is the transmittance of the output mirror. The reason we used this model is that it is mathematically more manageable than other more realistic models. Some spatiotemporal instabilities obtained from this model (e.g., supermode beating, switching from one transverse pattern to another with symmetry breaking, and bistabilities) qualitatively approximate what

have been observed in our He-Xe laser. Hence this simple model may be sufficient to reveal some basic physics about laser dynamics. Nevertheless, in our previous studies [11,12], the lowest frequency at which spatial patterns pulse was always *greater* than the smallest cavity frequency spacing. The pulsations at frequencies much lower than the intermode beat frequency were not found in that work.

We think that the previous failure to simulate the observed low-frequency pulsations using the model was most probably caused by the cavity-modal frequency spacings of that model, which increase linearly with the indices of the modes. Since two-dimensional laser models have equally spaced frequencies for their transverse modes and since experimentally the combined effects of astigmatism, transverse losses, and inhomogeneous spectral broadening tend to slightly shift the resonant frequencies, we decide to adjust by hand the frequencies of the cavity modes in the following way:

$$\omega_{n,c}=\omega_{0,c}+\kappa(a_1 n+\varepsilon n^2)\ , \tag{3}$$

where $a_1=a\pi^2$ and ε is $\ll a_1$. Therefore the frequency spacing between adjacent cavity modes becomes

$$\omega_{n+1,c}-\omega_{n,c}=\kappa a_1+\kappa(2n+1)\varepsilon\ . \tag{4}$$

The second term on the right-hand side of Eq. (4) represents a slight shift from equal frequency spacing. We begin our simulations with the initial state of the system in the fundamental transverse mode ($n=0$). Weak Gaussian random perturbations are given to all higher-order transverse modes. The highest-order transverse mode used in our numerical calculation is the mode $n=15$.

B. Parameters most affecting low-frequency pulsations

We first examine the effect of $\gamma_\parallel$ on the transverse dynamics of the system. Since the natural linewidth of the 3.51-μm transition in xenon, $\Delta\nu_{\mathrm{Xe}}$, is 4.6 ± 0.1 MHz [32] and the observed low frequencies of intensity pulsations are of this order of magnitude, we wondered whether there is a connection between the natural linewidth of the medium and low-frequency pulsations. In the model, the relaxation rate of population inversion, $\gamma_\parallel$, can be taken to be $\pi\Delta\nu_{\mathrm{medium}}$. Given that the frequency spacing between transverse cavity modes, $\Delta\nu_T$, is much greater than $\Delta\nu_{\mathrm{Xe}}$ ($\Delta\nu_{\mathrm{Xe}}$:$\Delta\nu_T$ is approximately 1:28 in the experimental laser), we run the computer code using different values of $\gamma'=\gamma_\parallel/\gamma_\perp$ from 1.0 to nearly 0 for $a_1=0.8$. The other parameters are $\kappa'(=\kappa/\gamma_\perp)=0.1$, $2C=3.5$, $\varepsilon=0.01$, and $\Delta=0.2$. This positions the fundamental mode slightly into the self-defocussing region of the gain medium. When $\gamma'\geq0.1$ ($\gamma'=1.0,0.5,0.1$), the original fundamental mode is stable. When $\gamma'\leq0.05$, ($\gamma'=0.05,0.01,0.009$), the laser switches to multimode operation and the total intensity $\langle I(t)\rangle$, which has been averaged over the transverse spatial domain [0,1] [$\langle I(t)\rangle=|f_0(t)|^2+\frac{1}{2}\sum|f_i(t)|^2$, $i>0$, where $|f_i|^2$ is the modal intensity of the ith transverse mode] pulsates periodically. The power spectra of $\langle I(t)\rangle$ show that the

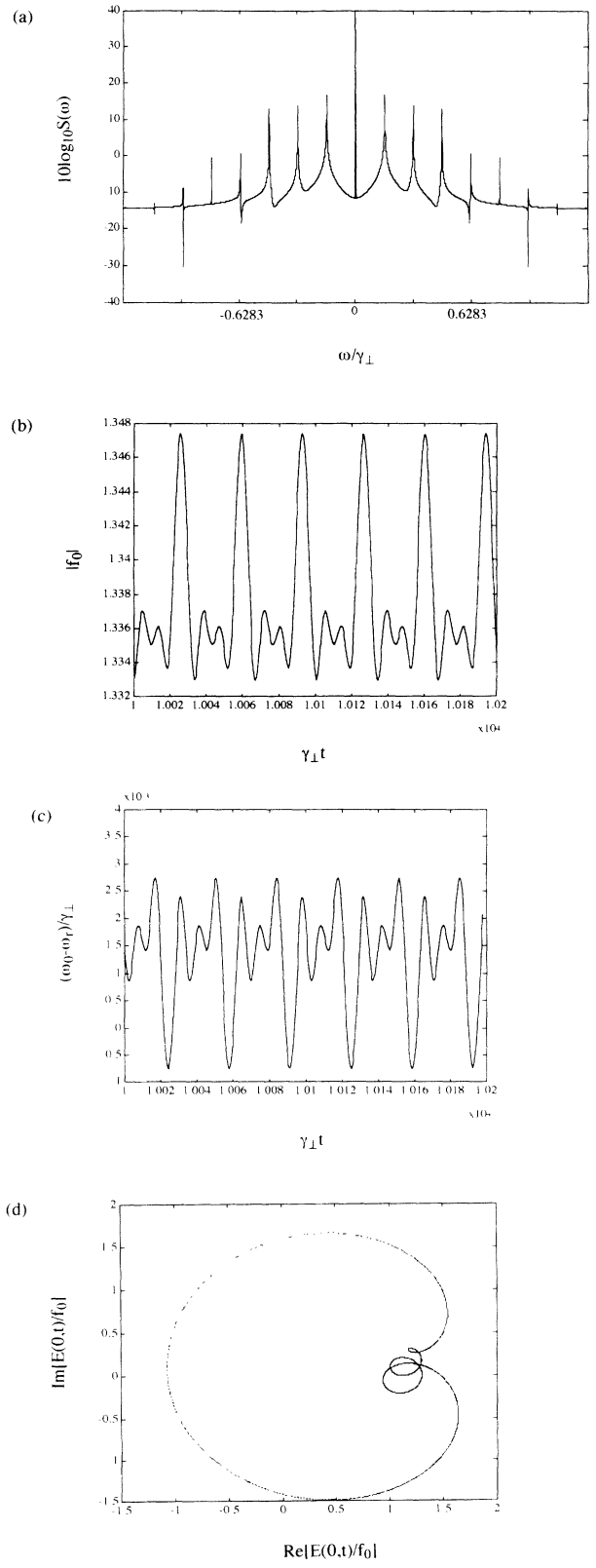

FIG. 6. Periodic, multimode operation for $\gamma'=0.01$, $\Delta=0.2$, $\kappa'=0.1$, $a_1=0.08$, $\varepsilon=0.01$, and $2C=3.5$. (a) Power spectra of $\langle I(t)\rangle$. (b) Modulus, $|f_0|$, and (c) frequency, $(\omega_0-\omega_r/\gamma_\perp)$, of the fundamental transverse mode which is the most dominant one vs time, $\gamma_\perp t$. ω_r is a reference frequency. (d) Phase diagrams of electric field at $x=0$ scaled by the fundamental mode.

lowest oscillation frequency is approximately twice the frequency spacing between the dominant modes. For example, when $\gamma'=0.01$, the strongest modes have indices $n=0-5$. Each mode lases nearly at its own modal frequency and $\langle I(t)\rangle$ periodically pulses at frequency $\omega/\gamma_\perp=0.169$ (which is very close to $2\kappa' a_1$) and its harmonics, as shown in Fig. 6. (From now on, all values of frequencies in the numerical simulations are in units of $\gamma_\perp$.) The modulus and frequency of each mode are also modulated at this frequency. This suggests that within this region of γ', frequency spacings are pulled or pushed to be equal and the operating modes are locked. As γ' is decreased to 0.007 or less, the transverse pattern and $\langle I(t)\rangle$ are still pulsing but the modes are not locked. The case that $\gamma'=0.003$ (now $2\gamma':\kappa' a_1=\Delta\nu_{\text{medium}}:\Delta\nu_T$ is approximately 1:14) is used as an example (Fig. 7). In the power spectrum of $\langle I(t)\rangle$, there are subpeaks around the peaks at the intermode beat frequencies 0, 0.157, (which is approximately $2\kappa' a_1$), 0.314, ... The lowest frequency in the power spectrum of $\langle I(t)\rangle$ is about 0.002, much less than the cavity-mode spacing and is of the order of γ'. Slowly varying envelopes are observed in the modal amplitudes and frequencies, indicating low-frequency AM and FM modulation. A similar low-frequency pulsation is also observed for $\gamma'=0.001$. When low frequencies appear in the power spectrum of $\langle I(t)\rangle$, the pulsations often become irregular (chaotic). This is shown clearly by the phase diagrams in Figs. 7(e).

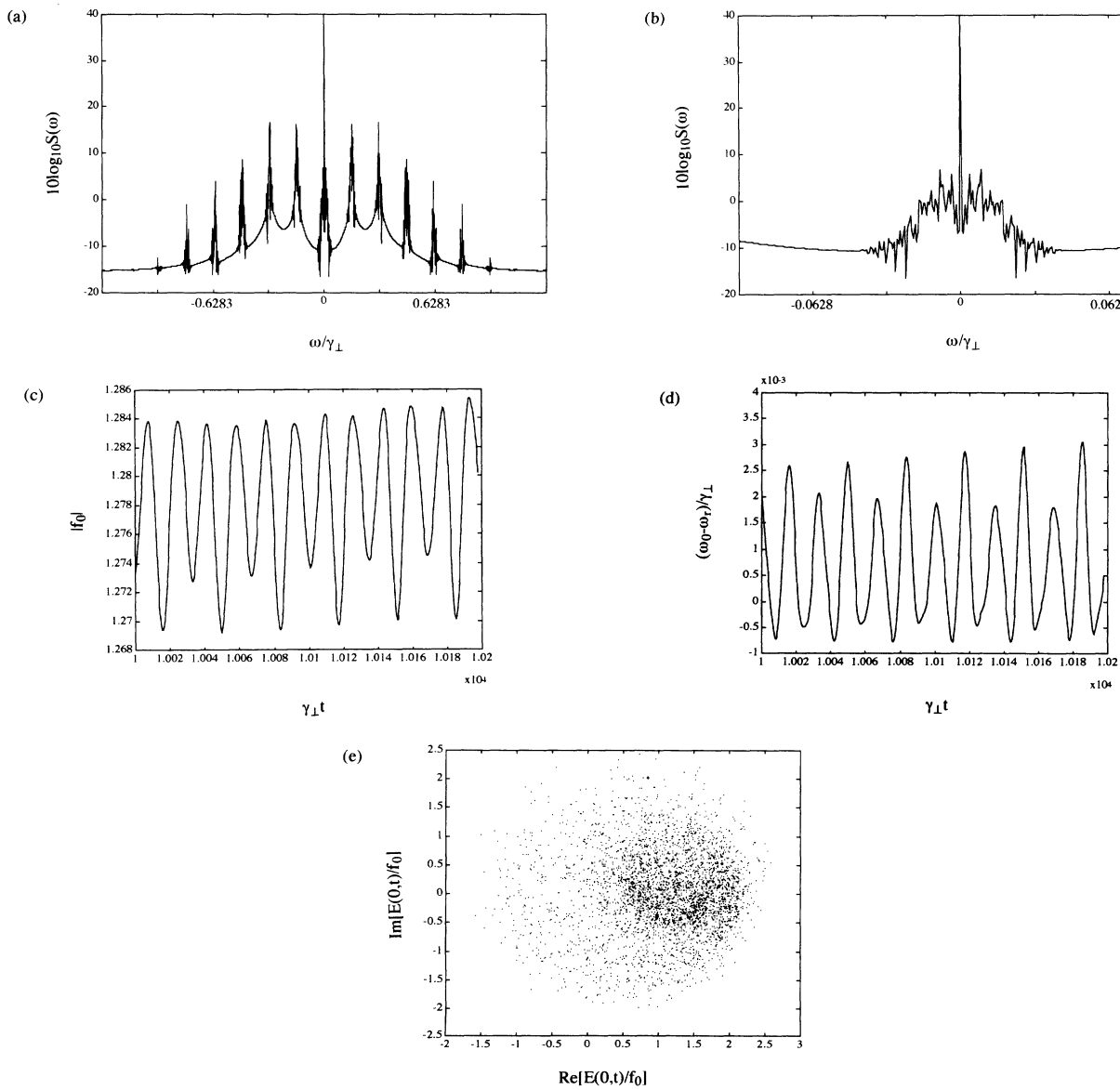

FIG. 7. Multimode operation with low-frequency pulsations for $\gamma'=0.003$. The other parameters are the same as those in Fig. 6. (a) Power spectra of $\langle I(t)\rangle$. (b) Details of low-frequency pulsation of (a). (c) Modulus and (d) frequency, $(\omega_0-\omega_r/\gamma_\perp)$, of the fundamental transverse mode which is the most dominant one vs time, $\gamma_\perp t$. ω_r is a reference frequency. (e) Phase diagrams of electric field at $x=0$ scaled by the fundamental mode.

As a second test of how these behaviors depend on the parameters of the model, the mode spacing parameter a_1 is changed while γ' is held at 0.003. The other parameters are the same as above. For $a_1=1.0$, 0.8, 0.6, and 0.4, many transverse modes operate simultaneously and low-frequency pulsations are always observed in the power spectra of $\langle I(t)\rangle$. As a_1 is decreased further, however, the low-frequency pulsations disappear. For $a_1=0.3$, only three modes—mode $n=4$, 5, and 8—become dominant. The combination tones are $2(\omega_5-\omega_4)_r/\gamma_\perp=0.075$ and its harmonics. Now $2\gamma':\kappa' a_1$ is 1:5.

Simulations were also done for other values of Δ. The detuning of the fundamental mode changes only the relative strengths of the modes, but the dynamical pattern is the same. For instance, different values of γ' are used for $\Delta=0.3$ and $a_1=1.0$. Low-frequency pulsations are observed for values of γ' from 0.003 to 0.05. When $\gamma'=0.1$, the modes are frequency locked and $\langle I(t)\rangle$ oscillates at $2\kappa' a_1$ and its harmonics, similar to the case in Fig. 6(a).

From these numerical results, it seems that the ratio of the population decay rate $\gamma_\parallel$ to the mode spacing κa_1 is the most important factor for appearance of low-frequency pulsations. When $\gamma'<\kappa' a_1$, we commonly observed low-frequency pulsations or unlocked multimode operations. These low-frequency pulsations are less sensitive to the pump parameter $2C$. The value of $2C$ was changed from 2.5 to 7.5 for $\gamma'=0.003$ and $a_1=0.8$ (with $\kappa'=0.1$, $\Delta=0.2$, and $\varepsilon=0.01$). There was no significant change in the low-frequency pulsations for different values of $2C$. The relaxation oscillation frequency $(\kappa'\gamma')^{1/2}$ (in units of $\gamma_\perp$) is much greater than the frequencies in the obtained low-frequency pulsation. Therefore the possibility that these low-frequency pulsations were triggered by or from relaxation oscillations can be excluded.

To see if Rabi oscillation has anything to do with the low-frequency pulsations, we again used $\Omega=(\gamma'\langle I\rangle)^{1/2}$ to estimate Ω, where $\langle I\rangle$ is the average value of $\langle I(t)\rangle$. For most results, the fundamental mode is the strongest mode. We have also calculated the Rabi frequency [which is $(\gamma'|f_0|^2)^{1/2}$] and the generalized Rabi frequency [which is $(\gamma'(|f_0|^2+\Delta^2)^{1/2}$] of the fundamental mode. However, their values are all greater than the low frequencies in the power spectra of $\langle I(t)\rangle$. Our conclusions is that the low-frequency pulsations are not caused by Rabi oscillation sidebands. This is in agreement with our experimental results.

C. Low-frequency pulsation and secondary beat frequency

It has been observed in a three-mode He-Ne 3.39-μm laser [15] that for some parameters, the three modes are not exactly equally spaced. The differences between different modal frequency spacings were termed secondary beat frequencies and these were much lower than intermode beat frequency. In our model, the secondary beat frequency between cavity modes is

$$\Delta\omega_c=(\omega_{n+1}-\omega_{n+1})_c-(\omega_{n+1}-\omega_n)_c$$
$$=2\kappa\varepsilon\ . \qquad (5)$$

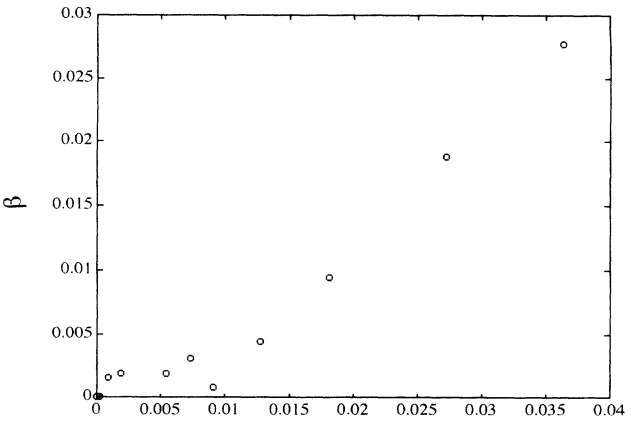

FIG. 8. The lowest frequency β of low-frequency pulsations vs the secondary beat frequency $\Delta\omega_s=2\kappa'\varepsilon/(1+\kappa')$, where $\gamma'=0.003$, $\kappa'=0.1$, $a_1=0.8$, $\Delta=0.2$, and $2C=3.5$.

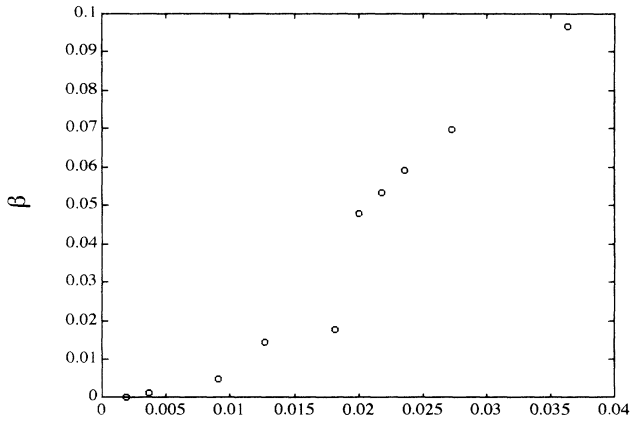

FIG. 9. The lowest frequency β of low-frequency pulsations vs the secondary beat frequency $\Delta\omega_s=2\kappa'\varepsilon/(1+\kappa')$, where $\gamma'=0.01$, $\kappa'=0.1$, $a_1=0.8$, $\Delta=0.2$, and $2C=3.5$.

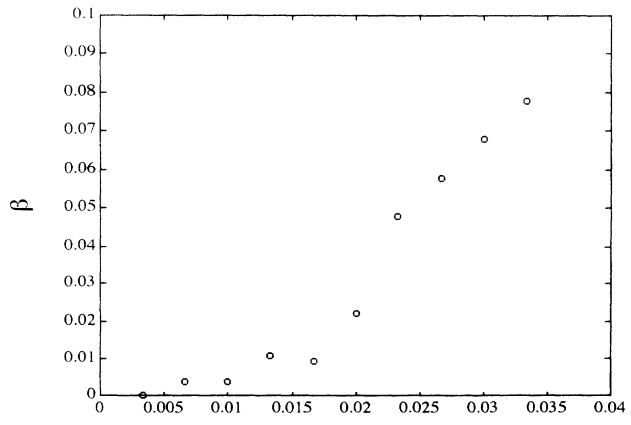

FIG. 10. The lowest frequency β of low-frequency pulsations vs the secondary beat frequency $\Delta\omega_s=2\kappa'\varepsilon/(1+\kappa')$, where $\gamma'=0.01$, $\kappa'=0.2$, $a_1=0.4$, $\Delta=0.2$, and $2C=3.5$.

TABLE II. Values of the lowest frequency in the power spectrum of $\langle I(t)\rangle$ within the nonlinear region of Fig. 8, for which $\gamma'=0.003$ and $\kappa'=0.1$.

β	$\Delta\omega_s$	$\kappa'\varepsilon$
0	0	0
0	0.000 18	0.0001
0.001 57	0.000 91	0.0005
0.001 88	0.001 82	0.001
0.001 88	0.005 45	0.003
0.003 14	0.007 27	0.004

Taking mode-pulling effects into account, the secondary beat frequency of lasing modes in units of $\gamma_\perp$ is

$$\Delta\omega_s=\frac{\Delta\omega_r}{\gamma_\perp}=\frac{2\kappa\varepsilon}{\kappa+\gamma_\perp}=\frac{2\kappa'\varepsilon}{1+\kappa'} . \tag{6}$$

The relation between the low-frequency pulsations and secondary beat frequencies is explored by varying the value of ε. Figure 8 illustrates the lowest pulsating frequency β in the power spectrum of $\langle I(t)\rangle$ vs $\Delta\omega_s$ for $\kappa'=0.1$, $\gamma'=0.003$, $\Delta=0.2$, $a_1=0.8$, and $2C=3.5$. The graph includes a linear part and a nonlinear part. When $\Delta\omega_s\geq 0.009$ (that is, $\kappa'\varepsilon\geq 0.005$), β is linearly proportional to $\Delta\omega_s$. The slope of this straight line is 0.98 and the intercept on the horizonal axis is 0.0081 ($\kappa'\varepsilon=0.0045$). The nonlinear part is for $0.000\,18<\Delta\omega_s<0.0091$ ($0.0001<\kappa'\varepsilon\leq 0.004$). Within this region β is of the order of $\kappa'\varepsilon$ or $\Delta\omega_s$, as shown in Table II. For $\Delta\omega_s<0.000\,18$ ($\kappa'\varepsilon\leq 0.0001$), the modes are frequency locked. $\langle I(t)\rangle$ oscillates at about $2\kappa' a_1$ and its harmonics only.

Figure 9 is β vs $\Delta\omega_s$ for $\gamma'=0.01$. The other parameters are the same as those in Fig. 8. There is also a linear part and a nonlinear part, but the slope of the linear part is 2.94, which is three times the slope in Fig. 8. Because the value of γ' for Fig. 9 is about three times that for Fig. 8, it is possible that the slope of the straight line part is proportional to γ'. The intercept on the horizontal axis is about 0.0038 ($\kappa'\varepsilon=0.0021$). The values of β in the nonlinear region are given in Table III and most of them are of the order of $\kappa'\varepsilon$. The upper limit of the nonlinear region is approximately $\Delta\omega_s=0.01$. The relaxation oscillation frequency is about 0.032; therefore it is not the origin of β for this case, either.

The influence of κ' on the relation between β and $\Delta\omega_s$ can be observed by comparing Fig. 9 and Fig. 10. For Fig. 10, $\kappa'=0.2$ and $a_1=0.4$. The other parameters are the same as used for Fig. 9. An interesting thing is that

TABLE III. Values of the lowest frequency in the power spectrum of $\langle I(t)\rangle$ within the nonlinear region of Fig. 9, for which $\gamma'=0.01$ and $\kappa'=0.1$.

β	$\Delta\omega_s$	$\kappa'\varepsilon$
0	0.0018	0.001
0.001 26	0.0036	0.002
0.005 0	0.0091	0.005
0.014 4	0.0127	0.007
0.017 6	0.0182	0.01

TABLE IV. Values of the lowest frequency in the power spectrum of $\langle I(t)\rangle$ within the nonlinear region of Fig. 10.

β	$\Delta\omega_s$	$\kappa'\varepsilon$
0	0.0033	0.002
0.0038	0.0067	0.004
0.0038	0.01	0.006
0.0107	0.0133	0.008
0.0094	0.0167	0.01
0.022	0.020	0.012

the slope of the linear part in Fig. 10 is 3.0, very close to that in Fig. 9. The intercept of the straight line is 0.0069, which is approximately twice that in Fig. 9. Values of β in the nonlinear region are shown in Table IV.

An interesting phenomenon is that the upper limits of the nonlinear regions—which is approximately $\kappa'\varepsilon=0.004$ in Fig. 8 ($\gamma'=0.003$), 0.01, in Fig. 9 ($\gamma'=0.01$) and 0.012 in Fig. 10 ($\gamma'=0.01$)—are close to the value of γ'.

IV. SUMMARY AND CONCLUSIONS

The numerical results show that the low-frequency pulsations can be interpreted as resulting primarily from the secondary beat frequency $\Delta\omega_r$. If the frequency shift parameter $\kappa'\varepsilon$ is greater than γ', the lowest frequency of pulsations, β, depends linearly on the secondary beat frequency. When $\kappa'\varepsilon<\gamma'$, β is of the order of $\kappa'\varepsilon$ or $\Delta\omega_r$. β becomes zero when $\kappa'\varepsilon$ is small enough, that is, when the modes are frequency locked. Rabi oscillations and relaxation oscillations do not contribute directly to these pulsations. However, when low-frequency pulsations appear, $\langle I(t)\rangle$ also pulsates at about $2\kappa' a_1$—which is about twice the cavity-mode frequency spacing—and its harmonics, as would be expected for modes separated by twice the minimal amount. We did not see these larger intermode beat frequencies in the homodyne spectra obtained in our experiment. This may be due to the finite bandwidth of the fast photodetectors and amplifier combinations. When the intermode beat frequency is higher than 100 MHz, it cannot be detected.

We have also shown that the ratio of γ' to the cavity-mode spacing is an important parameter for transverse dynamics in a laser. When $\gamma'>\kappa' a_1$, the laser is likely to operate on a single mode. Apparently, when γ' is sufficiently decreased, spatial hole burning is not "washed out" rapidly enough and the laser tends to switch to multimode operation in the form of pattern alternation at the low frequency of the second-order beats. So the laser is more likely to switch to multimode operation and low-frequency pulsation occurs. γ' appears to provide the locking band of each individual mode as frequency-locked or single-mode operation appears when the second-order beat frequency is reduced to less than this amount.

ACKNOWLEDGMENT

H. Lin would like to thank L. M. Narducci for providing the computer code used in Ref. [8], which has been adapted for these studies.

[1] J. A. Fleck, Jr. and R. E. Kidder, J. Appl. Phys. **36**, 2327 (1966).
[2] A. F. Suchkov, Zh. Eksp. Teor. Fiz. **49**, 1495 (1965) [Sov. Phys. JETP **22**, 1026 (1966)].
[3] L. W. Casperson and A. Yariv, Appl. Phys. Lett. **12**, 355 (1968).
[4] F. Hollinger and Chr. Jung, J. Opt. Soc. Am. B **2**, 218 (1985); **6**, 1013 (1990).
[5] M.-L. Shih, P. W. Miloni, and J. R. Ackerhalt, J. Opt. Soc. Am. B **2**, 130 (1985).
[6] L. A. Lugiato and M. Milani, J. Opt. Soc. Am. B **2**, 15 (1985).
[7] L. A. Lugiato, F. Prati, L. M. Narducci, P. Ru, J. R. Tredicce, and D. K. Bandy, Phys. Rev. A **37**, 3847 (1988).
[8] L. A. Lugiato, C. Oldano, and L. M. Narducci, J. Opt. Soc. Am. B **5**, 879 (1988).
[9] L. A. Lugiato, F. Prati, L. M. Narducci, and G.-L. Oppo, Opt. Commun. **69**, 387 (1989).
[10] H. G. Solari and R. Gilmore, J. Opt. Soc. Am. B **7**, 828 (1990).
[11] H. Lin and N. B. Abraham, Opt. Commun. **79**, 476 (1990).
[12] H. Lin and N. B. Abraham, J. Opt. Soc. Am. B **8**, 2429 (1991).
[13] M. Brambilla, F. Battipede, L. A. Lugiato, V. Penna, F. Prati, C. Tamm, and C. O. Weiss, Phys. Rev. A **43**, 5090 (1991); **43**, 5114 (1991).
[14] D. H. Auston, IEEE J. Quantum Electron. **QE-4**, 420 (1968); *ibid.* **QE-4**, 471 (1968).
[15] N. J. Halas, S. N. Liu, and N. B. Abraham, Phys. Rev. A **28**, 291 (1983).
[16] C. O. Weiss and H. King, Opt. Commun. **44**, 59 (1982).
[17] C. O. Weiss, A. Godone, and A. Olafsson, Phys. Rev. A **28**, 892 (1983).
[18] R. Hauck, F. Hollinger, and H. Weber, Opt. Commun. **47**, 141 (1983).
[19] F. Hollinger, Chr. Jung, and H. Weber, Opt. Commun. **75**, 84 (1990).
[20] Chr. Jung and F. Hollinger, Opt. Commun. **95**, 103 (1992).
[21] D. J. Biswas and R. G. Harrison, Phys. Rev. A **32**, 3835 (1985).
[22] Chr. Tamm, Phys. Rev. A **38**, 5960 (1988).
[23] W. Klische, C. O. Weiss, and B. Wellegehausen, Phys. Rev. A **39**, 919 (1989).
[24] J. R. Tredicce, E. J. Quel, A. M. Ghazzawi, C. Green, M. A. Pernigo, L. M. Narducci, and L. A. Lugiato, Phys. Rev. Lett. **62**, 1274 (1989).
[25] C. Green, G. B. Mindlin, E. J. D'Angelo, H. G. Solari, and J. R. Tredicce, Phys. Rev. Lett. **65**, 3124 (1990).
[26] E. J. D'Angels, C. Grenn, J. R. Tredicce, N. B. Abraham, S. Balle, Z. Chen, and G. L. Oppo, Physica D **61**, 6 (1992).
[27] N. Yu, R. K. Defreez, D. J. Bossert, G. A. Wilson, R. A. Elliot, S.-S. Wang, and H. G. Winful, Appl. Opt. **30**, 2503 (1991).
[28] R. S. Gioggi and N. B. Abraham, Phys. Rev. A **29**, 1304 (1984).
[29] J. R. Tredicce (private communication).
[30] A. E. Siegman, *Lasers* (University Science Books, Mill Valley, CA 1986).
[31] H. Risken and K. Nummedal, J. Appl. Phys. **39**, 4662 (1968); L. W. Hillman, J. Krasinski, R. W. Boyd, and C. R. Stroud, Jr., Phys. Rev. Lett. **52**, 1605 (1984); B. Segard, W. Sergent, B. Macke, and N. B. Abraham, Phys. Rev. A **39**, 6029 (1989).
[32] L. M. Hoffer, T. H. Chyba, and N. B. Abraham, J. Opt. Soc. Am. B **2**, 102 (1985).

(a)

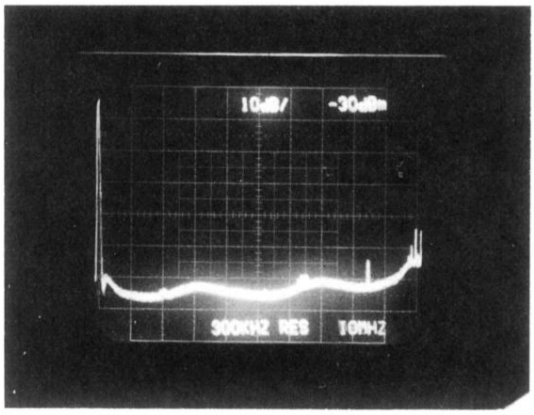

S(ν) (10 dB/div)

ν (10 MHz/div)

(b)

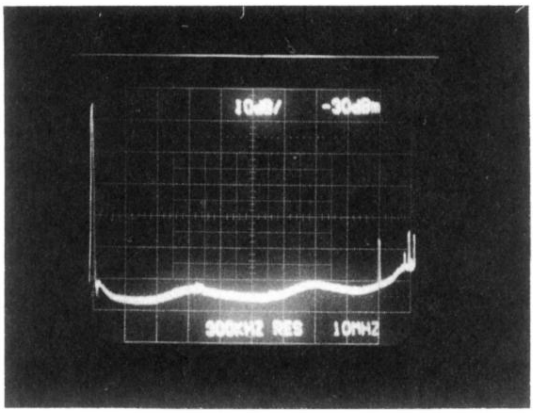

S(ν) (10 dB/div)

ν (10 MHz/div)

FIG. 3. Examples of homodyne and heterodyne spectra of intermode beating of the laser. (a) The intermode beat frequency (sharper peak) $f=90$ MHz and the two heterodyne beat nets ν_{B1} and ν_{B2} are -34 and 56 MHz, respectively. (b) $f=85$ MHz; ν_{B1} and ν_{B2} are -65 and 20 MHz, respectively. Horizontally, one grid in the picture is 10 MHz. The peaks at 100 MHz are due to electronic noise.

(a)

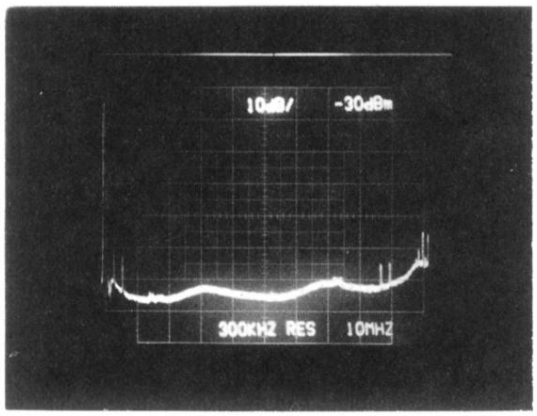

S(ν) (10 dB/div)

ν (10 MHz/div)

(b)

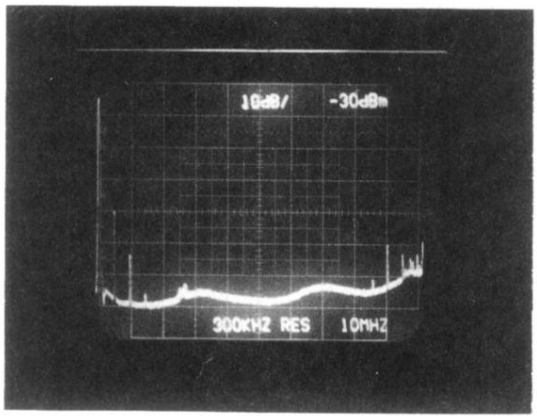

S(ν) (10 dB/div)

ν (10 MHz/div)

FIG. 4. Examples of homodyne and heterodyne spectra of low-frequency pulsation of the laser. Both low frequencies and intermode beat frequencies can be observed in (a) and (b). There are three heterodyne beat notes in (a), indicating that three modes are lasing. No intermode beat frequencies appear in (c) and (d).

(c)

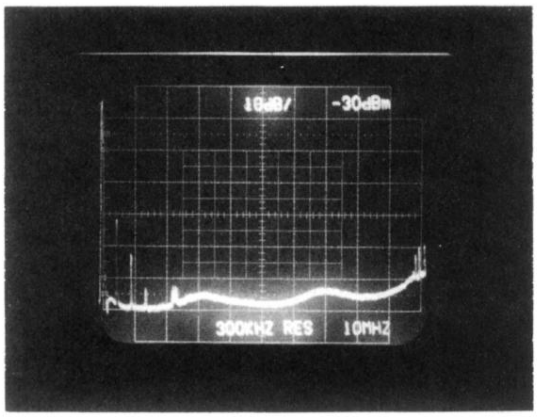

S(ν) (10 dB/div)

ν (10 MHz/div)

FIG. 4. (*Continued*).

(d)

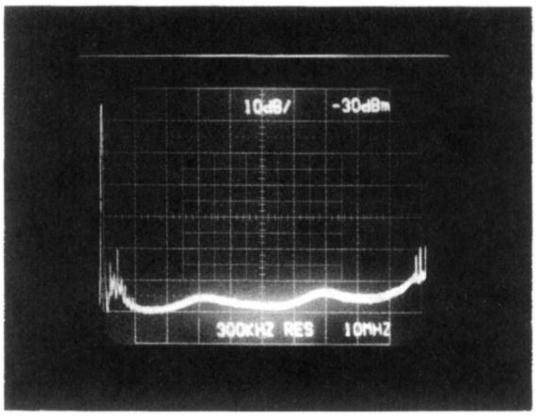

S(ν) (10 dB/div)

ν (10 MHz/div)